

# Quantum dynamics of vibrational excitations and vibrational charge transfer processes in $H^+ + O_2$ collisions at collision energy 23 eV<sup>†</sup>

SAIESWARI AMARAN<sup>#</sup> and SANJAY KUMAR\*

Department of Chemistry, Indian Institute of Technology Madras, Chennai 600 036

<sup>#</sup>Present address: The Fritz Haber Research Centre and The Department of Physical Chemistry, Hebrew University of Jerusalem, Jerusalem, Israel 91904

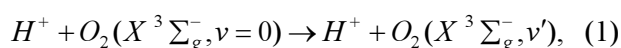
e-mail: sanjay@iitm.ac.in

**Abstract.** Quantum mechanical study of vibrational state-resolved differential cross sections and transition probabilities for both the elastic/inelastic and the charge transfer processes have been carried out in the  $H^+ + O_2$  collisions at the experimental collision energy of 23 eV. The quantum dynamics has been performed within the vibrational close-coupling rotational infinite-order sudden approximation framework employing our newly obtained quasi-diabatic potential energy surfaces corresponding to the ground and the first excited electronic states which have been computed using *ab initio* procedures and Dunning's correlation consistent-polarized valence triple zeta basis set at the multireference configuration interaction level of accuracy. The present theoretical results for elastic/inelastic processes provide an overall agreement with the available state-selected experimental data, whereas the results for the charge transfer channel show some variance in comparison with those of experiments and are similar to the earlier theoretical results obtained using model effective potential based on projected valence bond method and using semi-empirical *diatomics-in-molecules* potential. The possible reason for discrepancies and the likely ways to improve the results are discussed in terms of the inclusion of higher excited electronic states into the dynamics calculation.

**Keywords.** Potential energy surface; ground state; excited state; inelastic vibrational excitation; vibrational charge transfer.

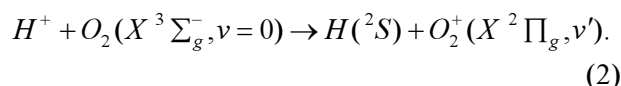
## 1. Introduction

The dynamics of energy transfer processes in proton–molecule collisions invariably evolves on highly coupled electronic potential energy surfaces (PES), and becomes quite complicated even in seemingly simple proton–diatom system. Despite great strides made in both experimental techniques and theoretical methodologies, state-to-state measurements and predictions on collision attributes in proton–molecule collisions have been reported only for some systems.<sup>1,2</sup> The  $H^+ + O_2$  system is one of the few proton–diatom systems for which state-selected experimental data exist for the inelastic vibrational excitation (IVE) channel,



at collision energy in the center-of-mass frame (c.m.),  $E_{c.m.} = 9.5$  eV.  $\nu$  stands for the vibrational state of the diatom. Good amount of state-selected

experimental data obtained from the molecular beam and the  $H^+/H$  energy-loss spectroscopy also exists at  $E_{c.m.} = 23$  eV for both the IVE channel, and the vibrational charge transfer (VCT) channel,



In the absence of accurate *ab initio* PESs for the electronic ground state (GS) and the excited states (ES) the earlier theoretical attempts have relied on semi-empirical or effective model descriptions of involved (quasi)diabatic PESs. Theoretical attempts to construct the quasi-diabatic PESs employing (i) the model effective potential procedures<sup>3</sup> based on the improved projected valence bond method and (ii) the semi-empirical *diatomics-in-molecules* (DIM) method<sup>4</sup> had been reported almost two decades ago. The early quantum dynamics results<sup>5,6</sup> within the vibrational close-coupling rotational infinite-order sudden approximation (VCC-RIOS) approach have been found to be in overall satisfactory agreement with those of experiments. However, quantitative discrepancies exist which still remain to be settled.

<sup>†</sup>Dedicated to the memory of the late Professor S K Rangarajan

\*For correspondence

In our previous study<sup>7</sup> we have presented a new set of *ab initio* adiabatic and quasi-diabatic PESs for the GS and the first ES of the  $H^+ + O_2$  collision system in the Jacobi coordinate,  $\mathbf{R}$ ,  $\mathbf{r}$  and  $\gamma$ , where  $\mathbf{R}$  is the proton distance from the center-of-mass (c.m.) of  $O_2$ ,  $\mathbf{r}$  is the internuclear distance of  $O_2$  and  $\gamma$  is the angular approach of  $H^+$  defined as  $\cos\gamma = \mathbf{R} \cdot \mathbf{r}$ . In the asymptotic limit the adiabatic GS and the first ES *ab initio* PESs correlate to  $H(^2S) + O_2(X^2\Pi_g^-)$  and  $H^+ + O_2(X^3\Sigma_g^-)$ , respectively. The adiabatic PESs have been computed at the multireference configuration interaction<sup>8–10</sup> (MRCI) level of accuracy employing Dunning's correlation consistent polarized valence triple zeta basis set.<sup>11</sup> The corresponding quasi-diabatic PESs have also been obtained employing *ab initio* procedure.<sup>12</sup> In ref 7, we have discussed various characteristics of PESs and carried out quantum dynamics calculations on the coupled quasi-diabatic PESs within the VCC-RIOSAs approach at  $E_{c.m.} = 9.5$  eV for the IVE and the VCT channels. At this collision energy, some state-selected experimental data exist<sup>2</sup> but only for the IVE channel. Our quantum dynamics calculations predict the experimental data very well for this channel. Plenty of state-selected experimental data<sup>13</sup> for both the IVE and the VCT channels exist at  $E_{c.m.} = 23$  eV in terms of differential cross section (DCS), vibrational transition probability,  $P_{0 \rightarrow \nu'}$  (from the initial  $O_2$  ( $\nu = 0$ ) state to any  $\nu'$  of  $O_2/O_2^+$ ) as a function of scattering angle ( $\theta_{c.m.}$ ), and average vibrational energy transfer. The experimental data for  $P_{0 \rightarrow \nu'}$  provide a crucial test for theoretical predictions since they depend on all the individual DCSs. Therefore, in order to further test the credence of the *ab initio* quasi-diabatic PESs we report our quantum dynamics study within the VCC-RIOSAs approach at  $E_{c.m.} = 23$  eV for  $P_{0 \rightarrow \nu'}$  as a function of  $\theta_{c.m.}$  for both the channels and compare the results with those of experimental<sup>13</sup> as well as earlier theoretical results.<sup>5,6</sup>

The paper is organized as follows: we briefly give the computational details of the dynamics in section 2. The results for  $P_{0 \rightarrow \nu'}$  for the IVE and the VCT channels are presented and discussed in section 3 along with the comparison with those of experimental as well as earlier theoretical results. A general discussion follows in section 4. A summary and conclusions are given in section 5.

## 2. Computational details

The relevant vibrational close-coupled equations have been given in ref. 7 with most of the numerical

details. Here, we give only the relevant numerical details at this collision energy. In order to have converged cross sections, 20 vibrational levels of the target diatom ( $O_2$ ) and 20 vibrational levels of the  $O_2^+$  system were included in the vibrational close-coupling equations. In order to get numerically converged results in terms of partial waves, for the elastic  $0 \rightarrow 0$  excitation of  $O_2$ , the maximum value of partial wave ( $l_{max}$ ) was 1200.

## 3. Results

In the molecular beam experiments<sup>13</sup> the state-to-state measurements for the IVE and the VCT processes were reported in terms of  $H^+$  and H-atom energy-loss peaks (spectra), respectively. The rotational excitations could not be resolved and their presence was inferred in terms of broadening of the energy-loss peaks. Also, in the experiments the value of  $P_{0 \rightarrow \nu'}$  (defined in (3)) were obtained as a ratio of the intensity of (energy-loss peak) that particular transitions to the grand total intensity of the IVE or the VCT channel. Therefore, following the earlier theoretical studies<sup>5,6</sup> the present theoretical values of  $P_{0 \rightarrow \nu'}$  were obtained from the rotationally summed vibrational DCSs. In quantum calculations DCS showed a lot of oscillatory structures as a function of  $\theta_{c.m.}$ , which arise mostly from the constructive and destructive interferences of the partial waves. Such undulatory structures could not be resolved in the experiments<sup>13</sup> where the angular resolution was reported to be of the order of  $\Delta\theta_{ab} = \pm 0.5$ . Therefore, we smoothed our data for the sake of clarity by folding them with a Gaussian distribution. The effect of smoothness is discussed in ref 7. In the present study, we report the results obtained from the smoothed DCSs.

### 3.1 Inelastic vibrational transition probability

The state-to-state (relative) transition probability  $P_{0 \rightarrow \nu'}$  for the IVE channel was obtained from the rotationally-summed DCS values

$$P_{0 \rightarrow \nu'}(\theta_{c.m.}) = \frac{d\sigma}{d\omega}(0 \rightarrow \nu')|_{\theta_{c.m.}} \left( \sum_{\nu=0} \frac{d\sigma}{d\omega}(0 \rightarrow \nu')|_{\theta_{c.m.}} \right)^{-1}, \quad (3)$$

$\nu'$  represents the vibrational states of  $O_2$ . It should be noted that the (relative)  $P_{0 \rightarrow \nu'}$  were calculated in

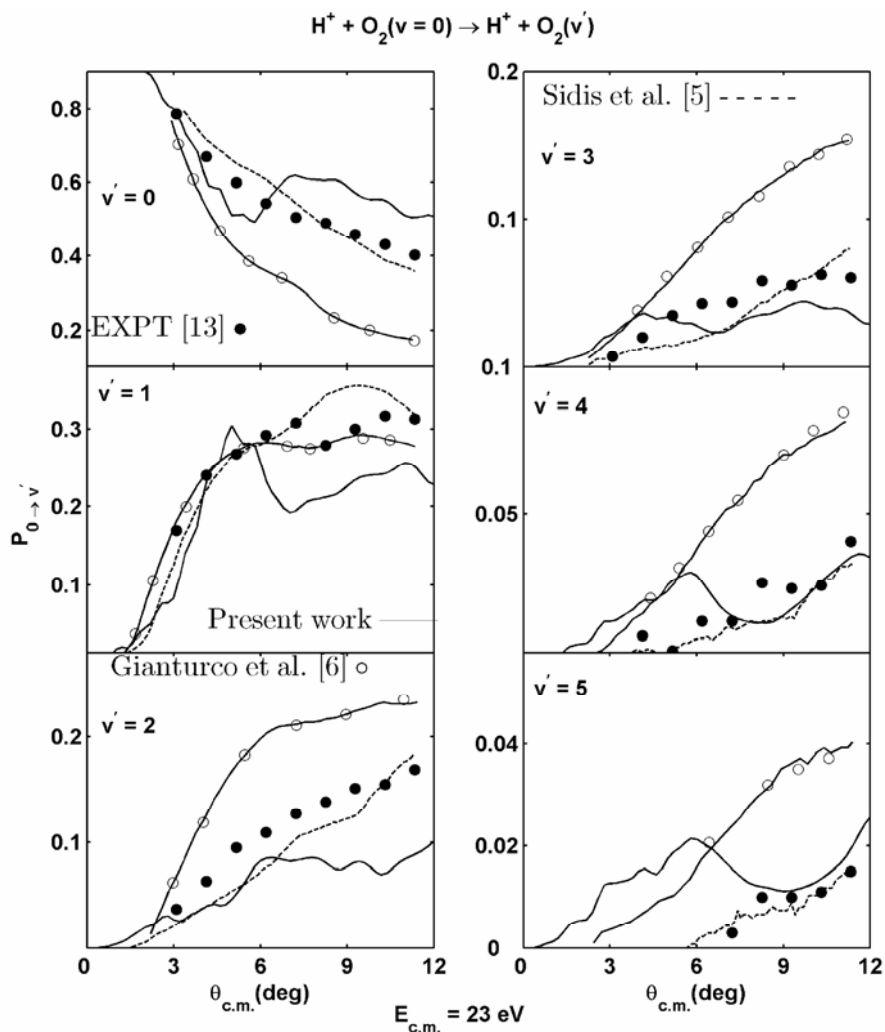


**Figure 1.** Transition probability  $P_{0 \rightarrow v'}$  (defined in (3)) for the IVE process,  $H^+ + O_2(X^3 \Sigma_g^-, v=0) \rightarrow H^+ + O_2(X^3 \Sigma_g^-, v')$ , as a function of  $\theta_{c.m.}$  at  $E_{c.m.} = 23$  eV. Experiment<sup>13</sup> ( $\bullet$ ), Present work (solid line), Sidis *et al.*<sup>5</sup> (dashed line) and Gianturco *et al.*<sup>6</sup> (line connecting open circles).

the similar manner as they were obtained in the experiments<sup>13</sup> and earlier theoretical calculations.<sup>5,6</sup> In figure 1,  $P_{0 \rightarrow v'}$  is shown as a function of  $\theta_{c.m.}$  for  $v' = 0-5$ . The corresponding theoretical data of Sidis *et al.*<sup>5</sup> and Gianturco *et al.*<sup>6</sup> are also reproduced there along with that of experiments of Noll and Toennies.<sup>13</sup> For the vibrationally elastic channel ( $0 \rightarrow 0$ ) (top left panel) the present calculations show a hump around  $\theta_{c.m.} \approx 8^\circ$  which appears to be severely quenched in the experiments as well as in the earlier theoretical calculations of Sidis *et al.*<sup>5</sup> and Gianturco *et al.*<sup>6</sup>. Overall, the results of Gianturco *et al.*<sup>6</sup> are underestimating for the elastic channel and overestimating for other vibrational excitations. On the other hand, the results of Sidis *et al.*<sup>5</sup> are better in

comparison with that of experiments. One can clearly see the differences in the dynamical outcomes which result due to the difference in the topologies and coupling of three different sets of quasi-diabatic PESs used in the theoretical calculations.

### 3.2 Vibrational charge transfer probability

The (relative)  $P_{0 \rightarrow v'}$  for the VCT channel was obtained from the rotationally-summed DCS values using (3) where  $v'$  refers to vibrational state of  $O_2^+$  and zero refers to the ground vibrational level of  $O_2$ . The computed  $P_{0 \rightarrow v'}$  are shown as a function of  $\theta_{c.m.}$  for  $v' = 0-5$  in figure 2 along with the theoretical data of Sidis *et al.*<sup>5</sup> and Gianturco *et al.*<sup>6</sup>. The experimen-

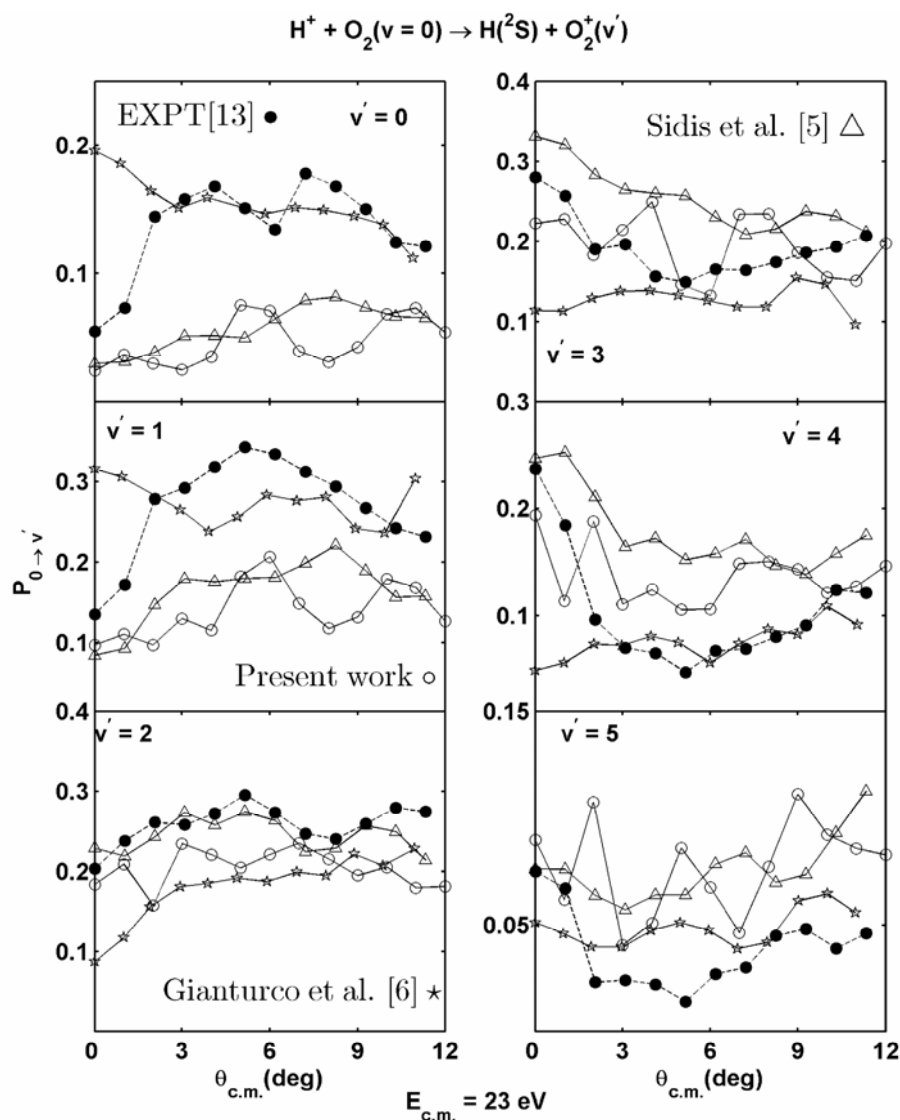


**Figure 2.** Transition probability ( $P_{0 \rightarrow v'}$ ) for the VCT process,  $H^+ + O_2(X^3 \Sigma_g^-, v=0) \rightarrow H(^2S) + O_2^+(X^2 \Pi_g, v')$ , as a function of  $\theta_{c.m.}$  at  $E_{c.m.} = 23 \text{ eV}$ . Experiment 13 ( $\bullet$ ); Present work ( $\circ$ ); Sidis *et al.*<sup>5</sup> ( $\Delta$ ) and Gianturco *et al.*<sup>6</sup> ( $\star$ ). See the text.

tal results of Noll and Toennies<sup>13</sup> (shown in solid black circles) are also reproduced there. The present calculations and those of Sidis *et al.*<sup>5</sup> and Gianturco *et al.*<sup>6</sup> are shown as open circles, open uptriangles and open stars, respectively. The experimental and earlier theoretical results were published as data points. However, for the sake of clarity and comparison we have presented them as line-connecting-points in figure 2. The experimental data are connected with dashed line. All the theoretical calculations show oscillatory structures. The experiments also show oscillatory patterns but they are not well marked. Overall, the relative magnitudes of the in-

dividual  $P_{0 \rightarrow v'}$  are satisfactorily predicted by the three sets of theoretical calculations. However, there are quantitative discrepancies and none of the theoretical calculations appear to be in overall quantitative agreement; it turns out that if a particular set of theoretical data predicts certain  $P_{0 \rightarrow v'}$  in good agreement with those of experiments then it fails to do so for other  $P_{0 \rightarrow v'}$ .

#### 4. General discussion

In this section, we discuss the likely cause of the discrepancy and the scope for the subsequent im-

provement. It would be instructive to compare first some salient characteristics of the GS ( $1^3A''$ ) and the first ES ( $2^3A''$ ) PESs used in earlier calculations of Gianturco *et al.*<sup>6</sup> and Sidis *et al.*<sup>5</sup> with those obtained in the present *ab initio* calculations. In figure 3, we compare the potential energy curves (PEC) for the GS and ESs as function of  $R$  with  $r = r_e$  (equilibrium bond length of  $O_2$ ) for  $\gamma = 45^\circ$ . Note that the  $r_e$  values obtained/used are slightly different in the present and earlier calculations. In the present calculations it is determined to be  $2.293a_0$  (Experiment. value,  $r_e(O_2) = 2.286a_0$ <sup>14</sup>). The PECs obtained by model projected valence bond calculations of Grimbert *et al.*<sup>3</sup> and by semi-empirical DIM calcula-

tions of Schneider *et al.*<sup>4</sup> are shown in figure 3(a) and (b), respectively. The present PECs obtained by the *ab initio* MRCI calculations are shown in figure 3(c). The  $3^3A''$  PEC is not available from calculations of Grimbert *et al.*<sup>3</sup>. For the sake of comparison the energy of  $2^3A''$  is arbitrarily set equal to  $1.0a_0$  at  $R = 7.0a_0$  in all the three sets. It is important to note that the ES PECs differ significantly. The first ES PEC ( $2^3A''$ ) of Grimbert *et al.*<sup>3</sup> remains purely repulsive, while in the DIM and present *ab initio* calculations it shows an avoided crossing with  $3^3A''$  state. Although the nature of avoided crossing is present in the DIM calculations they differ noticeably in comparison with the present *ab initio* calculations. The corresponding diabatic PECs obtained in the calculations of Grimbert *et al.*<sup>3</sup> have also been reproduced in figure 3a. The quasi-diabatic PECs obtained in the present calculations involving only the  $1^3A''$  and  $2^3A''$  states are also shown in figure 3c. The topology of (both the adiabatic and the quasi-diabatic)  $2^3A''$  state of Grimbert *et al.*<sup>3</sup> is markedly different as compared to that of the present calculations. However, overall, the computed  $P_{0 \rightarrow \nu'}$  values of Grimbert *et al.*<sup>3</sup> appear to predict the experimental data comparatively satisfactorily.

It is clear from the *ab initio* calculations that the  $3^3A''$  state is also expected to play a role in the dynamics. In fact, the ESs exhibit strong interactions among themselves. This is illustrated in terms of adiabatic PECs involving three and four states in figure 4a and c, respectively. Therefore, one expects that the topology and the associated coupling strengths of the quasi-diabatic  $2^3A''$  state would change with the inclusion of  $3^3A''$  and  $4^3A''$  states. In order to see the effect we have analysed the characteristics of the quasi-diabatic PECs obtained with the quasidiabatization of three- and four-electronic states, and they are shown in figures 4b and 4d, respectively. The topology of the quasidiabatic PEC of the first ES ( $2^3A''$ ) changes from two-state to three-state diabaticization (see figure 3c) showing mostly a repulsive behaviour as shown in the model effect potential calculations of Grimbert *et al.*<sup>3</sup>. One can also see that the topology of the quasi-diabatic  $V_{22}^d$  PEC which asymptotically correlates to the IVE channel,  $H^+ + O_2(X^3\Sigma_g^-, \nu=0)$ , undergoes little changes with two-, three- and four-state quasidiabatization. Note that the quasi-diabatic PECs  $V_{11}^d$  asymptotically correlate to the VCT channel,  $H(^2S) + O_2(X^2\Pi_g)$ . Similarly,  $V_{33}^d$  and  $V_{44}^d$  asymptotically correlate to  $H(^2S) + O_2(^4\Pi_u)$  and

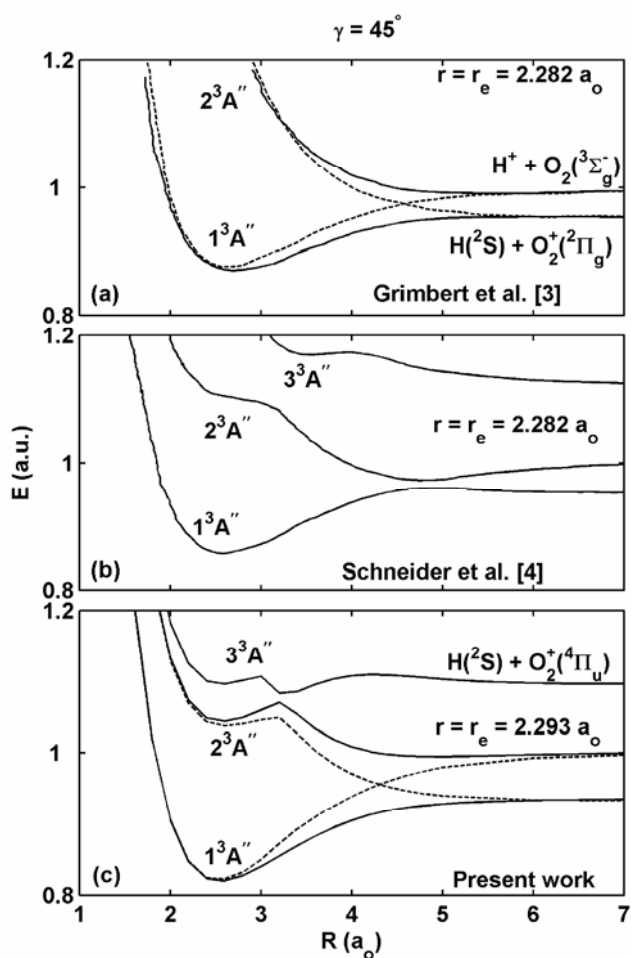


**Figure 3.** Comparison of the adiabatic potential energy curves (PECs) as a function of  $R$  with  $r = r_e$  for  $\gamma = 45^\circ$ . (a) Grimbert *et al.*<sup>3</sup>; (b) Schneider *et al.*<sup>4</sup>; (c) Present work. For the sake of comparison the energy of the adiabatic  $2^3A''$  state is arbitrarily set equal to  $1.0$  (a.u.) at  $R = 7.0a_0$ . The diabatic PECs involving  $1^3A''$  and  $2^3A''$  states have also been shown as dashed lines in (a) and (c). See the text.

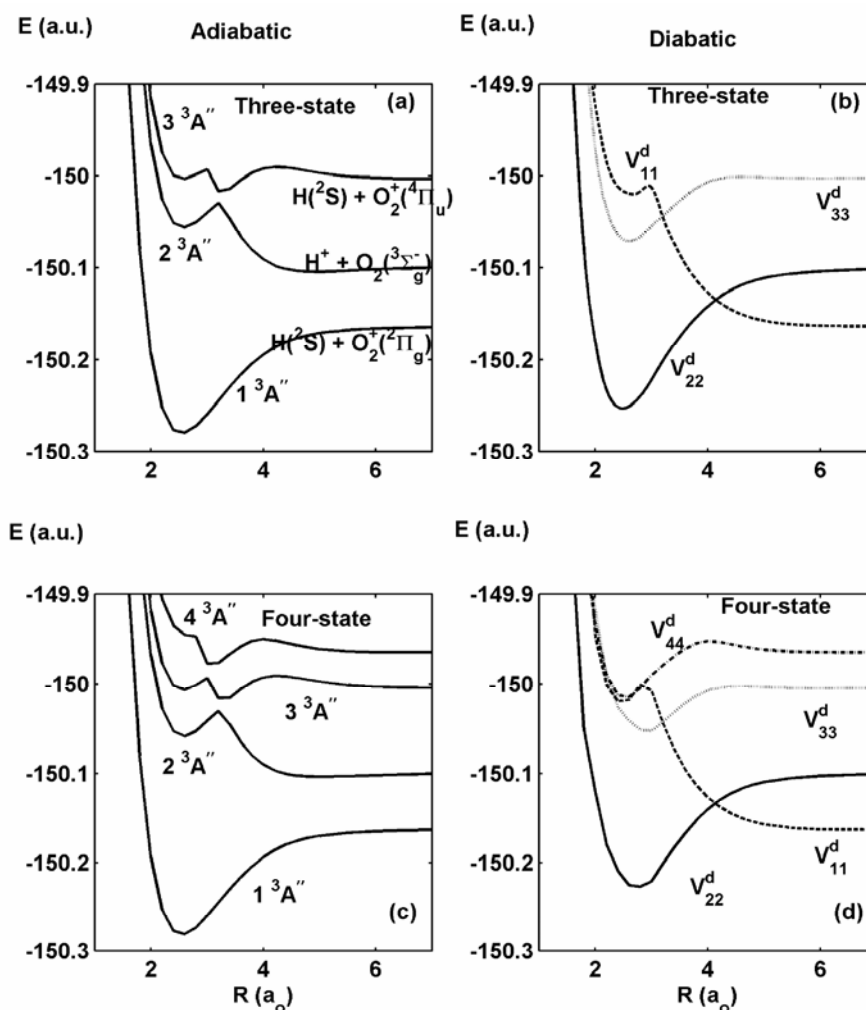


**Figure 4.** Adiabatic and diabatic PECs for the  $\text{H}^+ + \text{O}_2$  system at  $\gamma = 45^\circ$  and  $\mathbf{r} = 2.293a_0$ . Adiabatic PECs for the (a) three-state and (c) four-state; Diabatic PECs for the (b) three-state and (d) four-state. The  $4\ ^3A''$  correlates to  $\text{H}(^2S) + \text{O}_2^+(1^2\Pi_u)$ .

$\text{H}(^2S) + \text{O}_2^+(1^2\Pi_u)$ , respectively. An analysis of the quasidiabatic potential matrix reveals that the coupling between the  $1\ ^3A''$  and  $2\ ^3A''$  states remains almost the same as in the case of two-state and three-state diabaticization. In the case of three-state diabaticization, the coupling potential magnitude between  $2\ ^3A''$  and  $3\ ^3A''$  states remains comparable in strength with those of  $1\ ^3A'' - 2\ ^3A''$  coupling, whereas the coupling potential magnitude between  $1\ ^3A''$  and  $3\ ^3A''$  states are comparatively small. Therefore, one expects changes in the collision attributes both for the IVE and the VCT channels when one performs dynamics on the three-coupled electronic states. However, these changes are expected to be quite significant for the VCT channel in comparison with those of the IVE channel. This explains why most of

the collision attributes of the IVE channel at lower collision energy ( $E_{\text{c.m.}} = 9.8\ \text{eV}$ ) in ref. 7 were satisfactorily reproduced in comparison with those of experiments. To a certain extent they are also reproduced in the present calculations at  $E_{\text{c.m.}} = 23\ \text{eV}$ , except that the present calculations show a hump in the plot of  $P_{0 \rightarrow v'}$  versus  $\theta_{\text{c.m.}}$  at  $\theta_{\text{c.m.}} \approx 8$  which appears to be severely quenched in the experiments and also in the calculations of Grimbert *et al.*<sup>3</sup>. At  $E_{\text{c.m.}} = 23\ \text{eV}$  even the  $4\ ^3A''$  state would be energetically accessible. Interestingly, the experiments of Noll and Toennies<sup>13</sup> do not report any charge transfer with the excited electronic states of  $\text{O}_2^+$ . It could be possible that there is very little probability for the outcomes for the excited charge transfer states;  $\text{H}(^2S) + \text{O}_2^+(1^4\Pi_u)$  and  $\text{H}(^2S) + \text{O}_2^+(1^2\Pi_u)$ . Never-

theless, the potential coupling arising from the inclusion of the  $3^3A''$  and  $4^3A''$  states are expected to influence the collision dynamics at close approaches of  $H^+$ . Therefore, the observed quantitative discrepancies are expected to be diminished with the inclusion of the  $3^3A''$  and  $4^3A''$  states into the dynamics study.

## 5. Summary and conclusion

An extensive and elaborate analysis of the dynamical attributes at  $E_{c.m.} = 23$  eV has been made by comparing the state-to-state transition probability for vibrational excitations for the IVE and the VCT channels with those reported from earlier theoretical calculations vis-à-vis the available experimental data. For the IVE channel, a hump around  $\theta_{c.m.} \approx 8^\circ$  is seen in the present calculations which is seen to be severely quenched in the experiments.

For the VCT channel, overall, the relative magnitudes of the individual  $P_{0 \rightarrow \nu'}$  are satisfactorily predicted by all the three sets of theoretical calculations. However, there are quantitative discrepancies and none of the theoretical calculations appear to be in overall quantitative agreement; it turns out that if a particular set of theoretical data predicts certain  $P_{0 \rightarrow \nu'}$  in good agreement with those of experiments it fails to do so for other  $P_{0 \rightarrow \nu'}$ .

The likely cause of discrepancies and scope for the subsequent improvement have been discussed in detail by analysing the characteristics of the adiabatic PECs of the low-lying electronic states (of  $^3A''$  symmetry). Also, an analysis of the characteristics of the quasi-diabatic PECs obtained involving the two-, three- and four-state quasidiabatization suggests marked topological changes in the diabatic PECs correlating to the VCT channel. The diabatic PECs correlating to the IVE channel also get altered to a certain extent. Hence, we believe that the observed quantitative discrepancies in the present calculations are expected to be diminished with the inclusion of the next higher excited electronic states

in the quantum dynamics calculations since they would be accessible energetically at the considered range of collision energies. It would be worthwhile to undertake quantum dynamics on three and/or four coupled electronic states for this system.

## Acknowledgements

This study was supported by a grant from Department of Science and Technology, New Delhi. The financial assistance by Indian Institute of Technology Madras in procuring MOLPRO software is also gratefully acknowledged.

## References

1. Niedner-Schatteburg G and Toennies J P 1992 *Adv. Chem. Phys.* **LXXXII** 553
2. Gianturco F A, Gierz U, and Toennies J P 1981 *J. Phys. B: At. Mol. Phys.* **14** 667
3. Grimbert D, Lassier-Givers B and Sidis V 1988 *Chem. Phys.* **124** 187
4. Schneider F, Zulicke L, DiGuacomo F, Gianturco F A, Paidarov'a I, and Pol'ak R 1988 *Chem. Phys.* **128** 311
5. Sidis V, Grimbert D, Sizun M and Baer M 1989 *Chem. Phys. Lett.* **163** 19
6. Gianturco F A, Palma A, Semprini E, Stefani F and Baer M 1990 *Phys. Rev.* **A42** 3926
7. Amaran S and Kumar S 2008 *J. Chem. Phys.* **128** 154325
8. Werner H-J and Knowles P J 1988 *J. Chem. Phys.* **89** 5803
9. Knowles P J and Werner H-J 1988 *Chem. Phys. Lett.* **145** 514
10. Knowles P J and Werner H-J 1992 *Theor. Chim. Acta* **84** 95
11. Dunning Jr T H 1989 *J. Chem. Phys.* **90** 1007
12. Simah D, Hartke B and Werner H J 1999 *J. Chem. Phys.* **111** 4523
13. Noll M and Toennies J P 1986 *J. Chem. Phys.* **85** 3313
14. Huber K P and Herzberg G 1979 *Molecular spectra and molecular structure IV. Contents of diatomic molecules* (Princeton NJ: VNR)